The LBT AO system on-sky results

S. Esposito[1], A. Riccardi[1], E. Pinna[1], A. Puglisi[1], F. Quirós-Pacheco[1], C. Arcidiacono[1], M. Xompero[1], R. Briguglio[1], G. Agapito[1], L. Busoni[1], L. Fini[1], J. Argomedo[1], P. Stefanini[1], P. Salinari[1], G. Brusa[2], D. Miller[2]

[1]Osservatorio Astrofisico di Arcetri, Largo E. Fermi 5, 50125 Firenze, ITALY
[2]Large Binocular Telescope Observatory, 933N Cherry Avenue, Tucson, USA

Abstract. The first LBT natural Guide Star Adaptive Optics system (FLAO#1) has been commissioned between May 2010 and June 2011. The system uses two key components namely the adaptive secondary mirror with 672 actuators and the pyramid sensor with up to 30x30 subapertures. During the on-sky commissioning the system reached very high performance for an 8m class telescope. Briefly, FWHM of 40mas and Strehl ratio higher than 90% have been measured in H band images together with contrast as high as 10^{-4} at 0.4 arcsec off axis. The paper describes the results achieved during the system commissioning in terms of SR vs. reference star magnitudes and achieved PSF contrast. Finally the paper briefly discusses the sky coverage achieved with FLAO#1 and compares the results with the sky coverage achieved by LGS AO systems.

1. Introduction

The Large Binocular Telescope [1] (LBT) uses two 8.4m optical trains, each one of them fully integrated with AO correction provided by the two Adaptive Secondary Mirror [2] (ASM) units each one having 672 actuators. The First-Light AO (FLAO) system [3], one per telescope optical train, is a Natural Guide Star (NGS) single conjugate AO system featuring a modulated pyramid Wave-Front Sensor (WFS) with a maximum pupil sampling of 30×30 subapertures. A so fine spatial sampling is new for astronomical AO typically working in a photon starving regime. The spatial sampling is difficult to be realized also because of the technical limitations imposed by the limited degrees of freedom available on wave-front correctors. In the compromise between correction performance and available star light, the efficiency of wave-front sensors plays a dominant role. In our system, the use of state-of-the-art devices such as the pyramid WFS and the adaptive secondary mirror offers the optimal playground for very high Strehl Ratio (SR) corrections on the bright end, and high efficiency use of reference starlight photons on the faint one. As we will show in this paper, we have obtained >80% correction @ 1.6 µm on a bright star (up to MR~9), and closed efficiently the loop on a ~17th magnitude star with ~15 photons per subaperture per frame (~500 in the whole pupil). The on-sky commissioning of the FLAO#1 system (installed on the right side of the telescope) started in May 2010 and was completed in the fall of 2011. The installation of the FLAO#2 system on the left side of the telescope started in August 2011. The two FLAO systems will provide AO correction on the bent-Gregorian focal stations serving the two spectro-imagers of LBT called LUCI1 and LUCI2 [4].

In this paper after a brief system overview, we present a summary of the on-sky performance of the FLAO#1 system using the data collected during the commissioning nights. Finally we will report some considerations about the sky coverage achieved by the LBT AO system and a short comparison with the sky coverage results achieved using an LGS AO system.

2. An Overview of FLAO system

The FLAO system uses two key components: an adaptive secondary mirror and a modulated pyramid sensor. The rationale behind the selection of those components is made up by several reasons. An adaptive secondary mirror allows us to (a) have a reduced number of reflections; (b) feature a large number of actuators; (c) attain a performance that has a low sensitivity to small numbers of failed actuators; (d) have a single DM that can be used for all LBT focal stations. On the other side, a modulated pyramid sensor allows us to: (a) have a larger sensitivity than a SH sensor in faint end; (b) have a reduced aliasing effect in bright end of SH; (c) have an easily adjustable subaperture size via on-chip binning; (d) use a small (80x80 pixel) CCD for 30x30 subapertures. Figure 1 shows the ASM unit and the Pyramid sensor board of the FLAO system.

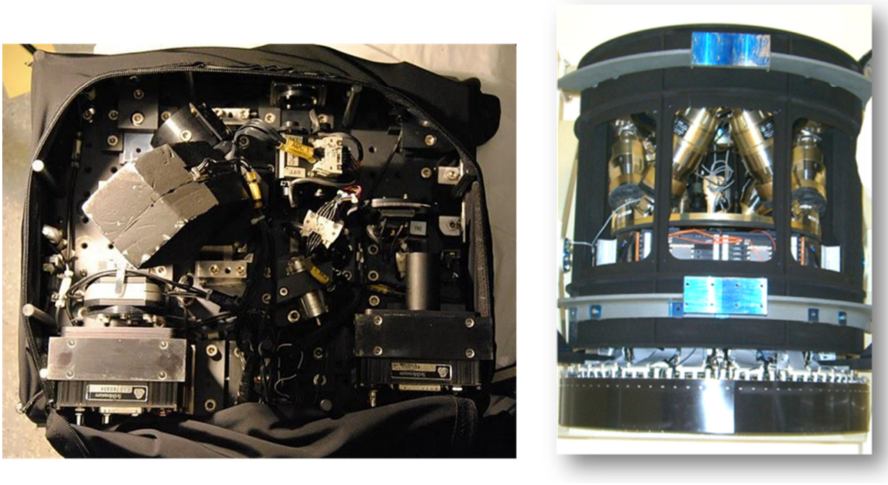

Figure 1. A picture of the FLAO system WFS board (left) and of the ASM unit (right).

An important feature of the FLAO system is that the temporal and spatial sampling of the WFS can be adjusted as a function of the star magnitude. In particular, the number of subapertures across the pupil diameter can be easily changed by choosing one of the on-chip CCD binning modes. In this way, the telescope pupil can be sampled with 30×30, 15×15, 10×10, or ~7×7 subapertures when using, respectively, binning modes #1, #2, #3, or #4. The sensitivity of the WFS can also be adjusted by means of the pyramid (circular) modulation. The typical system parameters used on sky as a function of the reference star magnitude are summarized in Table 1. Also in this table are listed the actual Read-Out Noise (RON) median values measured for each system configuration.

Table 1. Typical system configurations used on sky as a function of the equivalent R-magnitude of the GS (M_R). The system parameters are: the binning mode, the temporal sampling frequency (f_s), the number of controlled modes (n_{mod}), and the pyramid modulation. Median RON values measured for each configuration are also listed.

M_R	Binning mode	*Pupil sampling (# subaps.)*	f_s (Hz)	n_{mod}	Pyr. mod. ($\pm\lambda_s/D$)	RON (σ_{e-})
$M_R \leq 8.0$	1	30×30	990	500	2.0	10.5
$M_R \leq 10.0$	1	30×30	990	400	3.0	10.5
$10.0 < M_R < 13.5$	2	15×15	$990 \leq f_s \leq 300$	153	3.0	6.4
$13.5 \leq M_R < 14.5$	3	10×10	$500 \leq f_s \leq 200$	66	6.0	4.5
$14.5 \leq M_R < 16.5$	4	~7×7	$400 \leq f_s \leq 100$	36	6.0	4.6
$16.5 \leq M_R < 18.0$	4	~7×7	100	10	6.0	4.6

3. Commissioning results

We will now present the performance of the FLAO#1 system as obtained using the data collected during the commissioning nights [5, 6]. It is interesting to note that the system configuration during most of these observations was completely automatic. In particular the AO system configuration is done initially by selecting the system parameters from the already shown configuration table using the expected reference star flux. Then after the star is acquired the real flux is measured and the AO parameters are updated if needed. Finally a modal gain optimization procedure is run closing the loop on the considered object. After this last step, the system gains are updated the loop is kept running and the images are acquired. The mentioned three steps require from 2 to 3 minutes depending on the star magnitude.

3.1. Strehl Ratio vs. flux and seeing

The SR was estimated from the long-exposure PSFs measured with the InfraRed Test Camera [7] (IRTC) using an H-band filter with an effective central wavelength of 1.60µm. Total integration times varied from ~30s for high-flux PSF measurements up to ~120s for the low-flux ones. The camera was operated in the narrow Field-of-View (FoV) mode with a pixel scale of 10 mas/pixel.

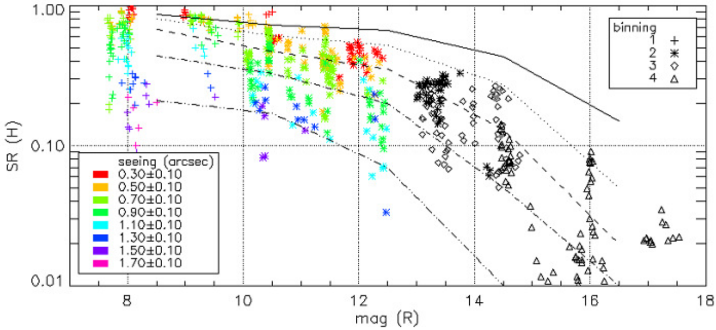

Figure 2. The plot reports the achieved SRs in H band as a function of the reference star magnitude. The color of the different points gives an estimate of the seeing values. Note that some of values are underestimated. The different lines refer to simulated performance for seeing values of 0.6, 0.8, 1.0, 1.2, 1.5 arcsec respectively.

Figure 2 summarizes the performance results attained by the FLAO#1 system. A total of 597 Strehl Ratio estimations at star magnitudes from ~7.5 to ~18 are shown in the plot. Seeing values estimated from AO real-time data [6] are coded in color. Points (MR >13) for which seeing values are strongly under-estimated with this method are shown in black. Figure 2 also indicates which system configuration (i.e. binning mode) has been used for each acquisition. Finally, the expected performances estimated from numerical simulations and for different seeing values (0.6", 0.8", 1.0", 1.2", and 1.5") are also shown in the plot as the 5 segmented curves. It is important to note that the measured SR values are in accordance with the simulated ones, showing that the FLAO#1 system meets the expected performance.

3.2. Effect of vibrations

The scatter of the SRs points reported in Figure 2 is mainly due to the different seeing conditions. This last dependence is found in Figure 3 where we plot SR vs seeing value for reference star magnitudes between 7 and 9. However some part of the scattering of Figure 2 has been identified as due to telescope vibrations. To get some quantitative informations let's consider again Figure 3.

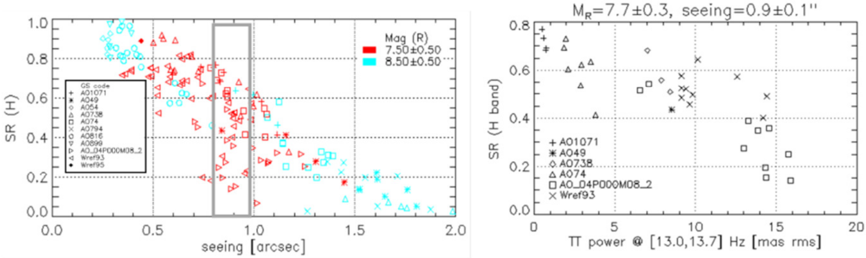

Figure 3. (Left) SR versus seeing for star magnitudes between 7.0 and 9.0. (Right) Effect of telescope vibrations on the measured SRs.

In the left side of Figure 3, the measured SR values are reported as a function of the seeing value. A rectangle identifies points measured with seeing values between 0.8 and 1.0 arcsec. The scatter of the SRs values is large and goes from 80% to 15%. The right side of the Figure reports the considered values plotted against the tip-tilt (TT) power found in a vibration line at ~13 Hz. The correlation between SRs and vibration power is quite remarkable. The 13 Hz vibration is related to the LBT telescope structure and in particular to the two swing arms that support the secondary and the tertiary mirrors. The LBT Observatory is developing a plan to reduce the amplitude of these vibrations. The vibrations are not always presents and vary in force mostly depending on the ground-layer wind speed and its direction with respect to the line of sight of the telescope. It has been clearly seen during the commissioning that looking off-wind delivers better performance than looking straight into the wind. This is true in particular when the sampling frequency of the system is less than ~500 Hz.

3.3. The achieved PSF contrast

One important result achieved with the LBT FLAO system is the image contrast reached in the corrected images, which is very important to detected faint point sources near bright stars, as required in searching for extra-solar planets. Figure 4 shows an example of a high-order corrected PSF in H band taken on June 25th 2010. Several images were acquired (saturated and non-saturated) to compute the PSF profile with the required resolution. The equivalent R magnitude of the GS (HD175658) is 6.5 and the estimated seeing value from real-time AO data oscillated between 0.6 and 0.8 arcsec. The AO loop was running at 1 kHz controlling 400 KL modes. Some residual TT vibrations @ 13.0-13.7Hz of 6 to 8 mas RMS were present. The estimated SR in H band is >80%.

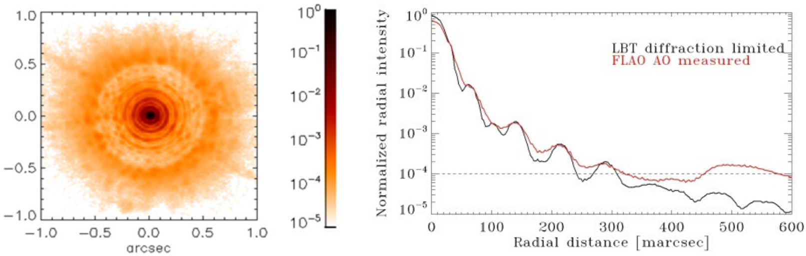

Figure 4 (Left) The high order corrected LBT PSF in H band. Several diffraction rings are seen plus the external AO control radius. (Right) The radial profile of the image showing a contrast better than 10^{-4}. Such a contrast is achieved without any coronograph.

Figure 4 also shows the radially-averaged profiles of the AO-corrected and the diffraction-limited PSFs. Note that a contrast better than 10^{-4} is achieved at a radial distance of ~0.4arcsec from the central peak. On the PSF image, it is possible to count up to 10 rings around the diffraction-limited core of 40mas FWHM, up to the turbulence residual halo (also known as the control radius) occurring at ~0.5arcsec. The characteristics of this image confirm on sky for the first time the deep annular region where the non-aliased correction offered by the pyramid sensor achieves the maximum contrast [8].

4. System sky coverage

The major limitation of the current AO systems with natural guide stars is the sky coverage, i.e., only targets near bright stars can be observed. This is particularly important for extragalactic targets, which rarely shown nearby bright stars. The LBT FLAO system provides significant corrections even with relatively faint stars, down to R~17, and this achievement boosts the sky coverage by a large fraction. To quantify this for a real, typical case, we consider as an example the catalog of 870 high-redshift Lyman Break Galaxies by Steidel el al. 2003[9], selected in 16 different, high galactic latitude fields.

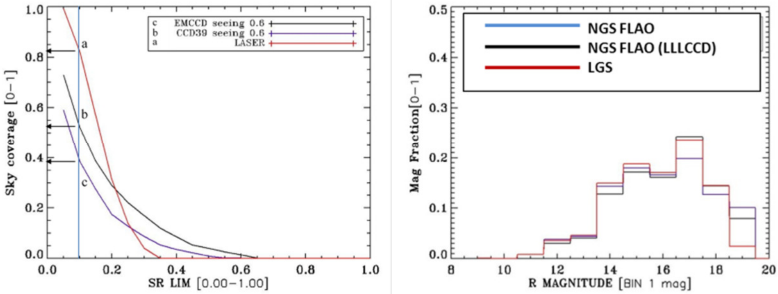

Figure 5 (left) the sky coverage achieved as a function of the required SR values. A,b and c lines refer to the FLBT AO, the LBT AO upgraded with an EMCCD and a laser system. The laser data are in agreement with results achieved at Keck telescope. (right) Magnitude of the reference star used in the computations for the three systems.

The actual system sky coverage depends on the required SR as shown in Figure 5 where we report the achieved sky coverage when a threshold SR value is required. Assuming a threshold SR of 10%, the sky coverage achieved by the FLAO system reaches the 40%, which is only a factor of 2 below what can be achieved by top level laser guide star system giving 80%. Moreover numerical simulation considering the LBT AO system upgraded to use an Electron Multiplied CCD has been done [10]. In this case, the sky coverage of the system is improved and is reported by the curve (b) in the plot. The 10% SR Sky Coverage is improved from 40% to 55% using the new CCD. Remarkably, the same sky coverage is obtained if SR>25% are requested, without the need of a more complex laser system.

5. Conclusions

The commissioning of the First Light AO system (FLAO#1) of the 2x8.4m LBT telescope has been completed in the period from June 2010 to August 2011. The achieved results —H-band Strehl Ratios higher than 80%, image contrast better than 10^{-4}, and loop closure down to 17.5 magnitude star— set a new standard for ground-based astronomical AO systems. At the same time these results show that adaptive secondary mirrors and pyramid sensors are mature technologies to be used in the design of future AO systems for 8m and ELT class telescopes. The LBT experience does show that a FLAO system upgraded with an EMCCD can achieve, in the case studied of extragalactic objects, a sky coverage of 54% comparable to the one obtained with an LGS of 84%. Moreover, a better sky coverage at SR higher than 25% can be achieved by the NGS system. These results, coupled with some of the limitations of LGS systems like cone effect and the need for low-order modes sensing with an NGS, suggest that the choice of using LGS systems instead of NGS systems, in astronomical application where anisoplanatism in the FoV is not the major concern, should be re-discussed.

6. References

1. Hill, J. M., "The Large Binocular Telescope," App. Opt. 49(16), D115-D122 (2010).
2. Riccardi, A. ; Xompero, M.; Briguglio, R.; Quirós-Pacheco, F.; Busoni, L.; Fini, L. ; Puglisi, A.; Esposito, S.; Arcidiacono, C.; Pinna, E.; Ranfagni, P; Salinari, P.; Brusa, G. ; Demers, R.; Biasi, R.; Gallieni, D., "The adaptive secondary mirror for the Large Binocular Telescope: optical acceptance test and preliminary on-sky commissioning results", Adaptive Optics Systems II. Edited by Ellerbroek, Brent L.; Hart, Michael; Hubin, Norbert; Wizinowich, Peter L. Proceedings of the SPIE, Volume 7736, pp. 77362C-77362C-12 (2010).
3. Esposito, S., Riccardi, A., Quirós-Pacheco, F., Pinna, E., Puglisi, A., Xompero, M., Briguglio, R., Busoni, L., Fini, L., Stefanini, P., Brusa, G., Tozzi, A., Ranfagni, P., Pieralli, F., Guerra, J. C., Arcidiacono, C. and Salinari, P. "Laboratory characterization and performance of the high-order adaptive optics system for the Large Binocular Telescope," App. Opt. 49(31), G174-G189 (2010).
4. Seifert, W., Appenzeller, I., Baumeister, H., Bizenberger, P., Bomans, D., Dettmar,R. J., Grimm, B., Herbst, T., Hofmann, R., Juette, M., Laun, W., Lehmitz, M., Lemke, R., Lenzen, R., Mandel, H., Polsterer, K., Rohloff, R. R., Schuetze, A., Seltmann, A., Thatte, N. A., Weiser, P. and Xu, W., "LUCIFER: a multi-mode NIR instrument for the LBT," Proc. SPIE 4841, 962–973 (2003).
5. Esposito, S., Riccardi, A., Fini, L., Puglisi, A. T., Pinna, E., Xompero, M., Briguglio, R., Quirós-Pacheco, F., Stefanini, P., Guerra, J. C., Busoni, L., Tozzi, A., Pieralli, F., Agapito, G., Brusa-Zappellini, G., Demers, R., Brynnel, J., Arcidiacono, C., and Salinari, P., "First light AO (FLAO) system for LBT: final integration, acceptance test in Europe, and preliminary on-sky commissioning results," Proc. SPIE 7736, 773609 (2010).
6. Esposito, S.; Riccardi, A.; Pinna, E.; Puglisi, A.; Quirós-Pacheco, F.; Arcidiacono, C.; Xompero, M.; Briguglio, R.; Agapito, G.; Busoni, L.; Fini, L.; Argomedo, J.; Gherardi, A.; Brusa, G.; Miller, D.; Guerra, J. C.; Stefanini, P.; Salinari, P., "Large Binocular Telescope Adaptive Optics System: new achievements and perspectives in adaptive optics", Astronomical Adaptive Optics Systems and Applications IV. Edited by Tyson, Robert K.; Hart, Michael. Proceedings of the SPIE, Volume 8149, pp. 814902-814902-10 (2011)
7. Foppiani, I., Hill, J. M., Lombini, M., Bregoli, G., Cosentino, G., Diolaiti, E., Herbst, T. M., Innocenti, G., Meschke, D., Miller, D. L., Rohloff, R. R., and Schreiber, L., "An instrument for commissioning the active and adaptive optics of modern telescopes: the Infrared Test Camera for the Large Binocular Telescope," Exp. Astron. (2011)
8. Vérinaud, C.; Le Louarn, M.; Korkiakoski, V.; Carbillet, M., "Adaptive optics for high-contrast imaging: pyramid sensor versus spatially filtered Shack-Hartmann sensor", Monthly Notices of the Royal Astronomical Society: Letters, Volume 357, Issue 1, pp. L26-L30, (2005)

9. Steidel, C. C., Adelberger, K. L., Shapley, A. E., Pettini, M., Dickinson, M. And Giavalisco, M., “Lyman Break Galaxies at Redshift z~3: Survey Description and Full Data Set”, Astrophys. J. 592(2), 728-754 (2003).
10. Carbillet, M., and Riccardi, A., “Low-light-level charge-coupled devices for pyramid wavefront sensing on 8 m class telescopes: what actual gain?”, App. Opt. 49(31), G167-G173 (2010).